ACKNOWLEDGMENT

This work was supported by NSF grant No. GK-455 and a National Aeronautics and Space Administration fellowship to John L. Deming.

NOTATION

C_p = heat capacity of solid
q = source energy per unit time
$\overline{q}$ = average source energy per unit time
Q = energy of the source
r = radial distance
R = radius of laser beam at the solid surface
R^* = dimensionless radius, r/R
t = time
T = temperature
T_1^* = dimensionless time, $T\rho C_p \pi R^3/2Q$
T_2^* = dimensionless time, defined by Equation (4)
w = weighting factor
z = axial distance
Z^* = dimensionless depth, z/R

Greek Letters

θ^* = dimensionless time, $4\kappa t/R^2$
$\overline{\theta^*}$ = dummy variable in Equation (4)
κ = thermal diffusivity
ξ = dimensionless variable, λR (3, 4)
ρ = density of solid

LITERATURE CITED

1. Anderson, J. E., and J. E. Jackson, *Welding J.*, 44, 1018 (1965).
2. Bahun, C. J., and R. D. Engquist, *Metals Eng., Quart.*, 27 (Feb., 1964).
3. Carslaw, H. S., and J. C. Jaeger, "Conduction of Heat in Solids," 2nd Ed. p. 258 to 60, Oxford Press, New York (1959).
4. Deming, J. L., MS thesis, Univ. Nebraska, Lincoln (1967).
5. ———, and L. C. Tao, and J. H. Weber, *AIChE J.*, 13, 1214 (1967).
6. Hampel, C. A., "Rare Metals Handbook," p. 635, Rheinhold Publ. Corp., New York (1954).
7. "Instruction Manual For Model K-150QP Laser," p. 1, Korad Corporation, Santa Monica, Calif. (1965).
8. Lindholm, U. S., E. J. Baker, and R. C. Kirkpatrick, *J. Heat Transfer*, 87, 49 (1965).
9. Ready, J. F., *Appl. Phys. Letters*, 3, 11 (1963).
10. Schmidt, A. O., I. Ham, and T. Hoshi, *Welding J. Res. Suppl.*, 44, 481 (1965).

Manuscript received October 24, 1967; revision received March 15, 1968; paper accepted April 26, 1968.

Laminar, Nonisothermal Flow of Fluids in Tubes of Circular Cross Section

E. B. CHRISTIANSEN and GORDON E. JENSEN

University of Utah, Salt Lake City, Utah

Numerical solutions of the equations of motion and energy are presented in the form of pressure-loss, flow-rate relationships for the laminar, nonisothermal flow of Newtonian and non-Newtonian fluids being heated and cooled in tubes at constant wall temperature. The flow properties are represented by a temperature-dependent form of the power law equation. The numerical results are shown to be in good agreement with experimental data for a wide range of fluid properties and flow conditions.

The heating and cooling of Newtonian and, especially, non-Newtonian fluids in laminar flow in tubes of circular cross section are becoming increasingly important in the chemical process industries. With few exceptions, presently available methods for the prediction of the pressure-gradient flow-rate relations for laminar, nonisothermal flow of Newtonian and non-Newtonian fluids in tubes of circular cross section employ the empirical Sieder-Tate type of corrections to introduce the effect of temperature on the flow of the fluid (*9, 14, 15*). While such methods are often satisfactory, extrapolation beyond the range of the data on which they are based may introduce serious error. Recently, a numerical solution of restricted equations of motion and energy which provides pressure-gradient flow-rate data for the laminar flow of non-Newtonian fluids being heated in tubes was reported (*5, 6*), in which a temperature-dependent form of the Ostwald-de Waele power law equation,

$$\tau = m[\dot{S} \exp(\Delta H^{\ddagger}/RT)]^n \qquad (1)$$

was used to represent the flow of the fluid. This equation is reported (*1, 12*) to represent quite accurately the flow of nonassociating Newtonian fluids ($n = 1$). Although, for pseudoplastic fluids ($n < 1.0$), Equation (1) predicts unrealistically high apparent viscosities at very low shear rates and unrealistically low apparent viscosities at very high shear rates, it correctly represents the flow of some non-Newtonian fluids over extended ranges of temperatures and shear rates (*2, 10*); and it represents the steady state flow of most non-Newtonian fluids over relatively narrow but significant and useful shear rate and tempera-

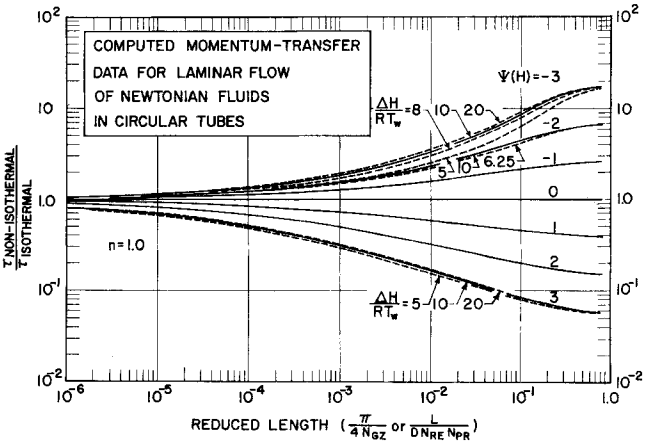

Fig. 1. Computed functions for Newtonian flow, $n = 1$. Positive values of $\Psi(H)$ represent energy transfer to the fluid, and negative values represent energy transfer from the fluid. The solid lines are for $\Delta H^{\ddagger}/RT_R = 10$. Dashed lines are included for $\Delta H^{\ddagger}/RT_R = 5$ to 20, when the function for these values differed by more than 2% from the function for $\Delta H^{\ddagger}/RT_R = 10$.

Gordon E. Jensen is with the United Technology Center, Sunnyvale, California.

ture ranges (*2, 4*).

In our work, the simplified equations of motion and energy were solved for flow [represented by Equation (1) for the case of cooling as well as for that of heating of the fluid] by numerical methods (*3, 7*) which differed from those previously used (*5, 6*), principally in that the higher order methods of integration were employed. The following assumptions were made:

1. The flow is steady state, and the convective terms in the equation of motion are negligible.
2. The flow is axisymmetric, and radial flow effects are negligible.
3. The fluid thermal conductivity, k; heat capacity, C; and density, ρ, are independent of temperature and pressure.
4. Isothermal flow is fully developed at the entrance to the tube section where heat transfer begins.
5. Thermal energy generation in the fluid by viscous dissipation or by any reaction is negligible.
6. Axial diffusion of momentum and energy is negligible.
7. The fluid is heated at constant wall temperature.

NUMERICAL PROCEDURES AND RESULTS

By means of the first, second, third, and sixth assumptions, the general equation of motion becomes

$$\frac{-\partial P}{\partial z} = \frac{1}{r}\frac{\partial (r\,\tau_{rz})}{\partial r} \tag{2}$$

In consequence of the second assumption, dP/dz is independent of r at any z; and under this condition, Equation (2) can be integrated to yield

$$-\frac{r}{2}\frac{dP}{dz} = \tau_{rz} = \frac{r}{R}\tau_{Rz} \tag{3}$$

From Equations (1) and (3), the velocity of any point z is

$$u = \left(\frac{\tau_{Rz}}{mR}\right)^{1/n}\int_r^R (r)^{1/n}\exp\left(-\Delta H^{\ddagger}/RT\right)dr \tag{4}$$

while the mass flow rate in the tube is

$$w = 2\pi\rho\int_0^R ur\,dr = 2\pi\rho R^3\left(\frac{\tau_{Rz}}{m}\right)^{1/n} I_2 = \text{constant} \tag{5}$$

By dividing Equation (4) by Equation (5), the local tube velocity as a function of temperature can be obtained (*3, 4, 7*):

$$u = \frac{w}{2\pi R^2\rho}\frac{I_1}{I_2} \tag{6}$$

The equation of energy, by assumptions 1, 2, 3, 5, and 6 and by combination with Equation (6), becomes, in reduced form

$$\frac{\partial T^+}{\partial z^+} = 2\pi\frac{I_2}{I_1}\left(\frac{1}{r^+}\frac{\partial T^+}{\partial r^+}\frac{\partial^2 T^+}{\partial r^{+2}}\right) \tag{7}$$

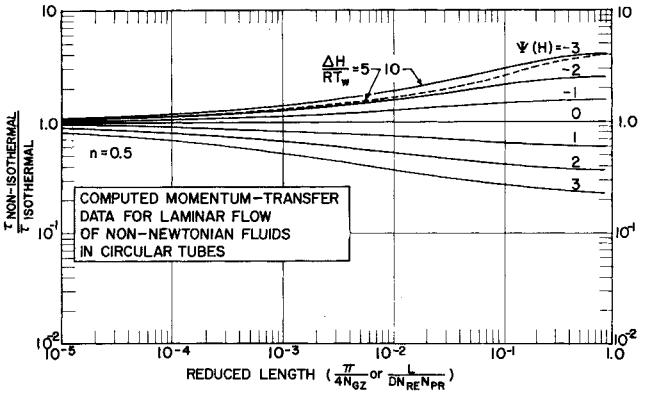

Fig. 2. Computed functions for non-Newtonian flow, $n = 0.5$, analogous to those of Figure 1.

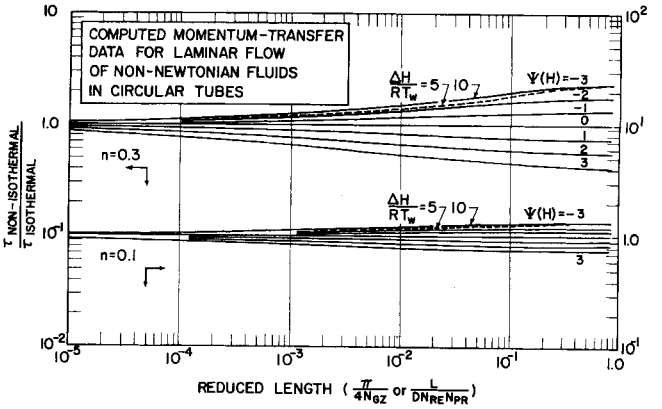

Fig. 3. Computed functions for non-Newtonian flow, $n = 0.3$ and 0.1, analogous to those of Figure 1.

Equation (7) was integrated by numerical methods (*7*) for constant tube-wall temperature.

In the finite-difference numerical computation, the tube flow field was represented by one hundred concentric sleeves of equal radial thickness and δz^+ length. Equation (7), with standard second-order finite-difference approximations in place of the partial derivatives, was used to obtain equations in terms of the initial and final temperatures for each of the flow elements, δz^+ long, starting at a given z^+. The resulting array of simultaneous equations was solved (*2, 4, 7*), by using a Crout reduction scheme (*8*), to obtain the temperatures at $z^+ + \delta z^+$. The velocities, $u(r)$, at $z^+ + \delta z^+$ were then computed by Equation (4) to comply with the temperature distribution and with the overall continuity and τ_{Rz} given by Equation (5). An explicit scheme was also tried; but the results were not discernibly different from those of the foregoing implicit scheme, and much more computer time was required. In consequence of the small mesh size and the independence of the results from mesh size, it is believed that the numerically determined results are within 1% of those which would be obtained by an exact solution of Equation (7).

The computations yield

$$\frac{\tau_{niso}}{\tau_{iso}} = f\left(n, N_{Gz}, \Delta H^{\ddagger}/RT_R, \frac{T_R - T_i}{T_i}\right) \tag{8}$$

Computed values of τ_{niso}/τ_{iso} are plotted vs. $\pi/4N_{Gz}$, with n, $\Psi(H) = \Delta H^{\ddagger}/RT_R\,(T_R - T_i)/T_i$, and $\Delta H^{\ddagger}/RT_R$ as parameters in Figures 1, 2, and 3. The computed functions for the case when the fluid is being heated are represented by positive values of $\Psi(H)$, and those for cooling are represented by negative values of $\Psi(H)$. The solid lines represent cases in which $\Delta H^{\ddagger}/RT_R = 10$, while the dashed lines represent those in which $\Delta H^{\ddagger}/RT_R = 5$ to 20, when the function for these values differed by more than 2% from the function for $\Delta H^{\ddagger}/RT_R = 10$.

DISCUSSION OF RESULTS

The computations, as illustrated in Figures 1, 2, and 3, emphasize the important influence of the temperature dependency of flow on pressure gradients for *nonisothermal* flow in tubes. These computations also demonstrate that this influence decreases markedly with decreasing values of n, as expected, and is importantly dependent on N_{Gz} or the reduced length.

In Figures 4 and 5 we have compared our computations with the experimental data of Vaughn (*15*), as reported by Metzner et al. (*9*), for aqueous 1.75% carbopol ($n_{avg} = 0.5$) and those of Hanks (*5*) for aqueous carbopol ($n = 0.5$ to 0.56) and CMC ($n = 0.60$ to 0.66). The relatively wider ranges of fluid properties and system

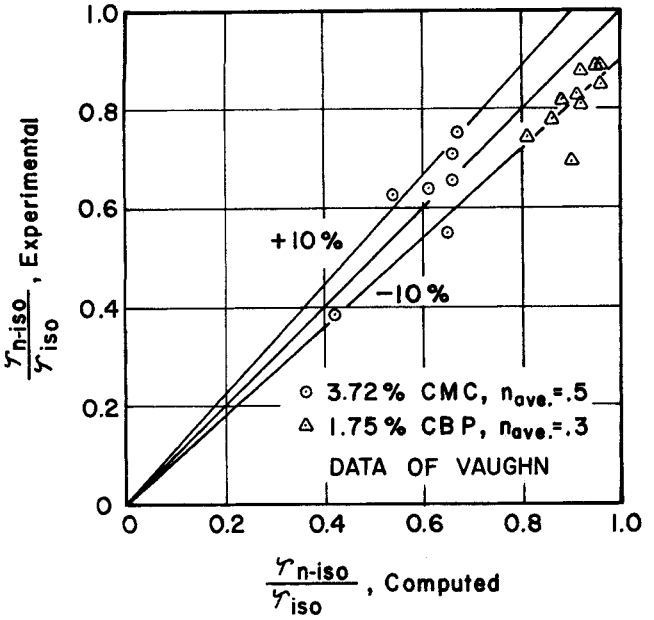

Fig. 4. Comparison of the experimental data of Hanks (5) for flow of non-Newtonian fluids in straight tubes of circular cross section, with the corresponding data predicted by means of the numerically computed functions.

parameters represented by these data are shown in Table 1. It should be pointed out that the data of Vaughn are not well represented by the power law and that the average values of n were used in the computations. The data of Vaughn can be more accurately represented by the Powell-Eyring equation (7, 13).

The mean deviation of the experimental data of Vaughn in Figure 4 from the predictions is 9%, but this deviation would be reduced if the point rather than the average values of n were used in the computation. Metzner, et al. (9) report mean deviations of 14 or 18% between their experimental and predicted pressure losses, by using an analog of the Poiseuille equation and the consistency at the bulk temperature plus a Sieder-Tate type correction or the consistency at a film temperature, respectively. These procedures used by Metzner, et al. do not account for the important dependency of the temperature effect on the reduced length, $L/(D\,N_{Re}\,N_{Pr})$, which is evident in Figures 1, 2, and 3. The mean deviation of the experimental data in Figure 5 from the computations is 6%, which is greater than that reported previously (6) for the same data compared with a similar computation. This difference appears to be largely the variance introduced when different individuals analyze the same data.

Although the restrictions of Equations (1) and (7) may, in some cases, be important, the results of the numerical solutions of Equation (2) for laminar, nonisothermal flow of fluids being heated or cooled in tubes, presented in Figures 1, 2, and 3, have been shown to adequately represent the experimental data for the nonisothermal, laminar flow of several non-Newtonian fluids, including some fluids which are mildly elastic. These solutions are adequate for numerous engineering purposes. They are more generally accurate if the Debra number, the temperature range, and the important shear-rate range are relatively small; these are also the conditions under which Equation (1) is more generally applicable.

ACKNOWLEDGMENT

The numerical program constitutes a part of a Ph.D. thesis by Gordon E. Jensen. The assistance of Dean Edwin Dallin, a graduate student in the Chemical Engineering Department and of the Computer Center at the University of Utah in making the computations is gratefully acknowledged. Financial support was provided by the National Science Foundation.

NOTATION

C = heat capacity, cal. g.$^{-1}$ °K.$^{-1}$
D = pipe diameter, cm.
$I_1 = \int_{r+}^{1} (r^+)^{1/n} \exp(-\Delta H^{\ddagger}/RT)\, dr^+$, dimensionless
$I_2 = \int_{0}^{1} I_1\, r^+\, dr^+$, dimensionless
k = thermal conductivity, cal. cm.$^{-1}$ sec.$^{-1}$ °K.$^{-1}$
L = length of heated tube, cm.
m = constant in Equation (1), dynes (sec.)^n (cm.)$^{-2}$
n = constant in Equation (1), dimensionless
N_{Gz} = Graetz number, wC/kL, where C and k are evaluated at the average film temperature, $T_R/2 + T_i/4 + T_o/4$, dimensionless
N_{Pr} = Prandtl number, dimensionless
N_{Re} = Reynolds number, dimensionless

TABLE 1. FLOW PROPERTIES OF THE FLUIDS AND FLOW PARAMETERS

Source	Fluid	n	$\Psi(H)$	Tube diameter (in.)	L/D	N_{Gz}
(9)	1.75% Carbopol	0.18-0.4	0.39 to 1.13	1.37	167	101 to 2,054
(9)	3.72% CMC	0.43-0.55	2.3 to 3.07	1.37	167	225 to 1,723
(5)	CMC-K	0.66	0.714 to 0.775	1.5	72	2,050 to 6,900
(5)	CMC-L	0.605	1.52 to 1.63	1	110	2,320 to 7,110
(5)	Carbopol-G	0.502	0.795 to 0.873	1.5	80	6,820 to 12,200
(5)	Carbopol-H	0.561	0.687 to 0.716	1	120	2,300 to 4,670

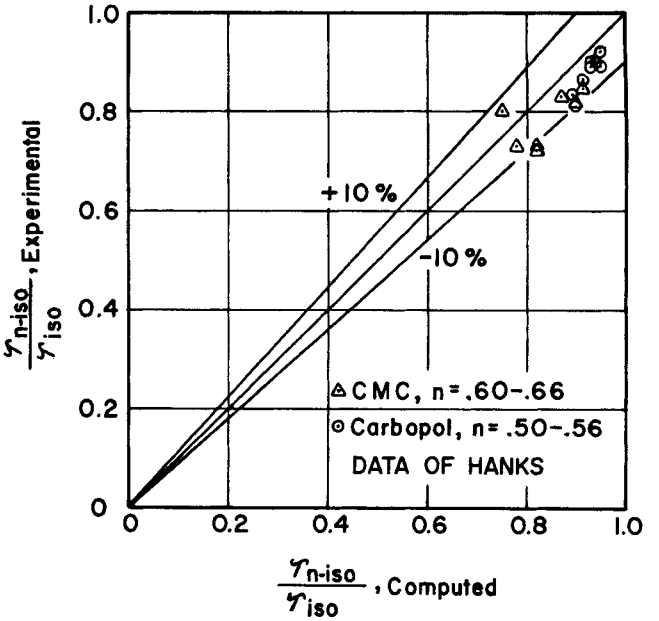

Fig. 5. Comparison of the experimental data of Vaughn (15) for flow of non-Newtonian fluids in straight tubes of circular cross section, with the corresponding data predicted by means of the numerically computed functions.

r = local radius, cm.
r^+ = reduced radius (r/R), dimensionless
R = Boltzman constant (cal./mole/°K.) or pipe radius (cm.)
$\dot{S}$ = strain rate, $-du/dx$ ($-du/dr$ for tube flow), sec.$^{-1}$
T = absolute temperature, °K.
T^+ = reduced temperature, $(T - T_i)/(T_R - T_i)$, dimensionless
u = local velocity, cm. sec.$^{-1}$
w = mass flow rate, g. sec.$^{-1}$
z = axial coordinate, cm.
z^+ = N_{Gz}^{-1}, $z\,k/w\,C$

Greek Letters

$\Delta H^{\ddagger}/R$ = constant in Equation (1), °K. [$\Delta H^{\ddagger}$ is interpreted (*11*) to be the activation energy for flow]
π = 3.1416
ρ = density, g. cm.$^{-3}$
τ = shear stress, dynes cm.$^{-2}$ (momentum flux)
$\Psi(H)$ = $(\Delta H^{\ddagger}/R)\,(1/T_i - 1/T_R)$, dimensionless

Subscripts

i = inlet
iso = isothermal
niso = nonisothermal
o = outlet
R = wall

LITERATURE CITED

1. Andrade, E. N. da C., *Endeavour*, **13**, 117 (1954).
2. Christiansen, E. B., and S. E. Craig, Jr., *AIChE J.*, **8**, 154 (1962).
3. ———, Gordon E. Jensen, and Fan-Sheng Tao, *ibid.*, **12**, 1196 (1966).
4. Craig, S. E., Jr., Ph.D. thesis, Univ. Utah, Salt Lake City (1959).
5. Hanks, R. W., Ph.D. thesis, Univ. Utah, Salt Lake City (1960).
6. ———, and E. B. Christiansen, *AIChE J.*, **7**, 519 (1961).
7. Jensen, Gordon E., Ph.D. thesis, Univ. Utah, Salt Lake City (1963).
8. Lapidus, L., "Digital Computation for Chemical Engineers," McGraw-Hill, New York (1962).
9. Metzner, A. B., R. D. Vaughn, and G. L. Houghton, *AIChE J.*, **3**, 92 (1957).
10. Peterson, A. W., Ph.D. thesis, Univ. Utah, Salt Lake City (1960).
11. Ree, T., and H. Eyring, *J. Appl. Phys.*, **25**, 793 (1955).
12. Reid, Robert C., and Thomas K. Sherwood, "Properties of Gases and Liquids," p. 203 McGraw-Hill, New York (1958).
13. Salt, D. L., N. W. Ryan, and E. B. Christiansen, *J. Colloid Sci.*, **6**, 146 (1951).
14. Sieder, E. N., and G. E. Tate, *Ind. Eng. Chem.*, **28**, 1429 (1938).
15. Vaughn, R. D., Ph.D. thesis, Univ. Delaware, Newark (1956).

Manuscript received March 29, 1967; revision received May 6, 1968; paper accepted May 9, 1968.

Mass Transport in Porous Materials under Combined Gradients of Composition and Pressure

ROBERT D. GUNN and C. JUDSON KING

University of California, Berkeley, California

An expression is derived for the analysis of gas-phase mass transport in porous media in the presence of gradients in pressure and mole fraction. The behavior of porous media is contrasted with that of capillary tubes. A continuous-flow diffusion and permeation apparatus was employed for studies of mass transport in a fritted glass diaphragm. Measurements were obtained at varying levels of pressure and cover both isobaric binary diffusion and the permeation of pure gases and gas mixtures. These experimental results and previous data obtained by Hewitt and Sharratt and by Mason, *et al.* bear out the form of the equation and successfully provide independent checks of the three constants necessary to characterize a given porous medium.

Gas-phase mass-transport phenomena in porous media are only partly understood for the situation in which mutual diffusion, Knudsen diffusion, and hydrodynamic flow all occur simultaneously. Nevertheless, these phenomena are important factors in the design of isotope separation equipment and nuclear reactors (*12, 13, 22, 23*), in predicting reaction rates in many catalysts (*38, 39*), and in the drying of porous materials (*18, 30, 44, 45*).

The study of transition-region diffusion in porous media can be divided into three major areas:

1. Purely diffusional mechanisms (isobaric conditions).
2. Combined diffusion and hydrodynamic flow (nonisobaric conditions).
3. Special phenomena such as surface flow, electroosmosis, etc.

Equations for isobaric diffusion have been derived by Scott and Dullien (*48*) and by Evans, Watson, and Mason (*14*). These relationships, which will be discussed later, have been verified experimentally as well (*21, 48*).

Nonisobaric mass transfer is considerably more complicated. A total pressure gradient superimposes Newtonian flow upon diffusion whenever the mean pore diameter of a porous body is comparable in size to or larger than the mean free path length of a gaseous mixture within that body. This situation, where Newtonian flow, Knudsen diffusion, and mutual diffusion all occur simultaneously, is the subject of this paper. The additional complications which are presented by surface diffusion or other special phenomena are not dealt with here.

Robert D. Gunn is presently with the University of Texas, Austin, Texas.